Journal of Engineering Mathematics, Vol. 8, No. 3, July 1974
Noordhoff International Publishing–Leyden
Printed in The Netherlands

Numerical studies for viscous swirling flow through annular diffusers

Part I. Method

C. M. CRANE

School of Mathematics, Computing and Statistics, City of Leicester Polytechnic, Leicester, England.

D. M. BURLEY

Department of Applied Mathematics and Computing Science, University of Sheffield, Sheffield, England.

(Received September 25, 1973)

SUMMARY

A method for finite difference computation of incompressible viscous swirling flow through annular diffusers is presented. Calculations (based on the steady-state Navier–Stokes equations including non-linear terms) are made to determine the distributions of stream-function, vorticity and swirl velocity. A description is given of a new method for determining the dynamic head and static pressure distributions. In addition evaluation of the various performance parameters is considered. Computational difficulties and the capabilities of the computer program developed to solve the problem are also discussed.

1. Introduction

In many rotodynamic machines such as turbines, pumps and compressors, flow in diffusers has considerable practical importance. By gradual expansion of the passage through which the fluid is flowing, a reduction in the velocity level together with an increase in static pressure can be achieved. In this way, kinetic energy is converted to pressure energy. As a result of the decreased velocity level, it is possible to reduce energy losses. However, the resulting flow is against an adverse pressure gradient and with this condition, the main flow is liable to separate from the boundary. Separation increases energy losses and leads to very non-uniform velocity profiles at exit and so the problem of designing diffusers that allow maximum static pressure rise without causing separation is very important. Decreasing energy losses and obtaining a good pressure recovery is by no means the only application of diffusers, but is one to which much research interest has been devoted.

Diffusers are encountered in a variety of shapes and sizes depending on the diffuser installation in question. Most experimentalists have concerned themselves with the simpler geometries such as straight walled two-dimensional, radial, conical or annular diffusers. In practical situations, of course, the actual diffuser shape is usually dictated to within certain limits by space and cost limitations.

A great deal of the research work on diffusers has been concerned with performance characteristics and design problems. Experimental diffuser studies are numerous in the literature. Performance charts have been plotted and comparisons made between the performance characteristics of two-dimensional, conical and annular diffusers [1], [2]. The effect of the inlet boundary layer and its importance in conical diffusers has been demonstrated [3]. More recently, interesting results with swirling inlet flow have been obtained [4], [5]. Theoretical attempts to predict diffuser flow and performance have, in the main, used boundary layer methods involving step by step solution of the boundary layer growth in an adverse pressure gradient. Studies of this type, for rotationally symmetric flow passages including conical diffusers, [6]–[8], have produced results whose agreement with experiment is most encouraging. An interesting analytical approach [9] for the case of certain annular diffusers uses a linearised vorticity method but assumes constant inlet and exit static pressure distributions.

One of the interests that motivated the present work was the nature of separation and the corresponding recirculating flow regions. Although by consideration of the shape factor [10] it is possible using boundary layer methods to predict separation, a study of the full recirculating regions is really beyond the scope of boundary layer methods. It therefore became necessary to solve the full Navier–Stokes equations including all the non-linear terms. To solve these equations in full generality is far beyond the scope of present day computers and so some compromise was necessary. The steady-state swirling axisymmetric case was chosen. Time dependent studies are feasible (by, for example, extending a method in [11]) but to deal with turbulence adequately was beyond the capabilities of the available computer. However, the case under consideration is important and as yet unexplored territory.

The diffuser geometry considered here is an annular diffuser having a conical outer casing and a cylindrical hub. This configuration is very similar to that used in the experimental study [5]. One of the main interests was the possible effect that a swirl velocity component in the fluid could have on the flow regime. Originally it was felt that swirl could critically affect separation. This surmise has indeed subsequently been proved correct by experiment [4], [5]. The hub of the diffuser was made capable of rotation so that swirl could be induced as well as introduced at inlet. To the authors' knowledge there have been no extensive theoretical studies of swirling diffuser flows.

The numerical procedure that has made the current computations possible employs "Upwind Differences", as introduced in [12] to approximate convection terms. The use of "Upwind Differences" theoretically detracts from the accuracy, but it does ensure that the matrices of coefficients of the sets of finite difference equations are unconditionally diagonally dominant thus promoting numerical stability especially at higher Reynolds numbers. Furthermore, "Upwind Differences" yield feasible solutions for some problems where central differences give physically unrealistic results.

2. Formulation of a problem

The investigations reported here have been restricted to annular diffusers consisting of a conical outer wall with a centrally placed cylindrical hub (see fig. 1) but the computer program developed for the problem is readily adapted for a much wider range of configurations. The equations governing the motion are, in dimensionless form

$$(V\cdot\nabla)V = -\nabla P + \frac{1}{R}\nabla^2 V \tag{2.1}$$

$$\text{div } V = 0 \tag{2.2}$$

The Reynolds number, R, is based on the inlet annulus width and the inflow velocity.

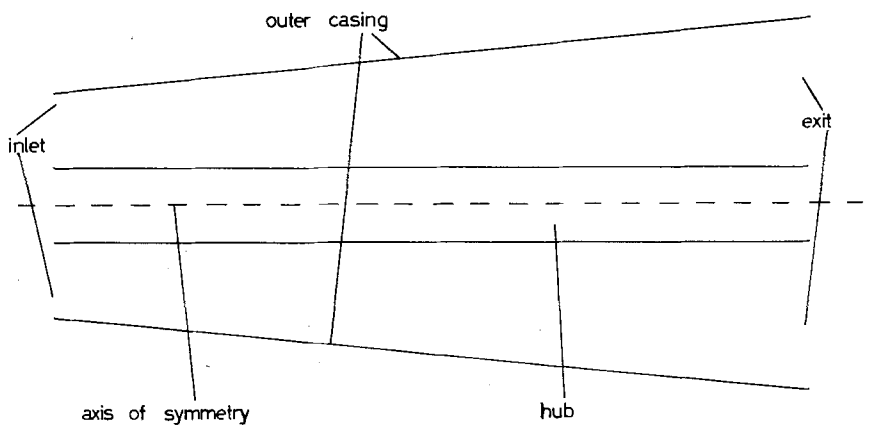

Figure 1. The diffuser geometry.

2.1. *The co-ordinate system*

The amount of computation involved in the implementation of the boundary conditions is dependent on the suitability of the co-ordinate system used. The spherical polar co-ordinate system is ideal for conical diffusers without a hub. However, this system is not so well suited to the present problem since the hub boundary would not lie along a co-ordinate line. The co-ordinate system derived for use here is a generalisation of the spherical polar co-ordinate system that allows all boundaries to coincide with co-ordinate lines. The details of the system are pictured in fig. 2. This system is ideally suited to a wide range of straight walled annular geometries.

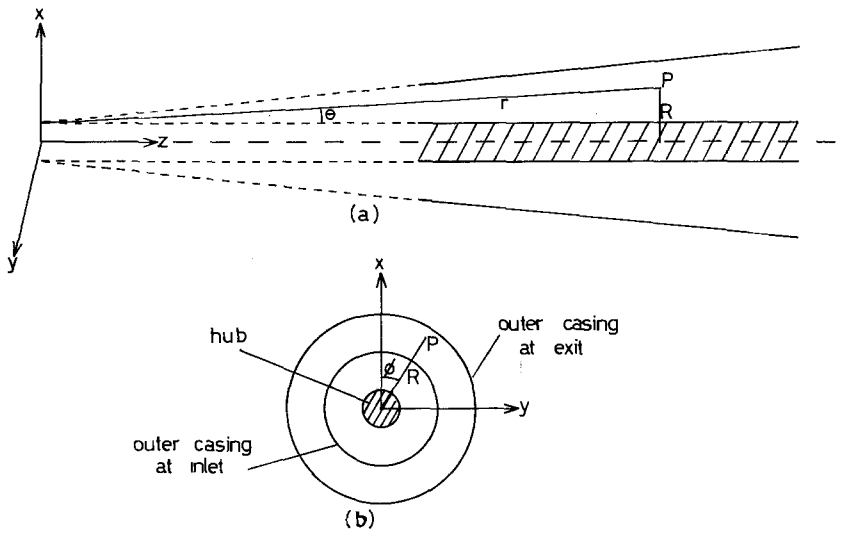

Figure 2. The co-ordinate system.

2.2. *Boundary conditions*

The inlet flow is known and on the walls, the "no slip" assumption gives the appropriate conditions. The major difficulty is the exit boundary. The authors are not aware of any completely satisfactory treatment of such a boundary. One difficulty is that the conditions clearly depend on whether the flow is fed into an infinite still medium, into a cylindrical tail pipe, or into any other fluid handling system. It is, however, not unreasonable to assume that the downstream conditions do not have too great an effect on the upstream behaviour. It was therefore decided to use the simplest reasonable boundary conditions necessary to ensure that a solution of the equations is possible. These conditions insist that the flow be radially directed (for r of fig. 2) at the exit: the nearest physical analogue is that of "free slip" guide vanes placed at the exit. The conditions are by no means perfect since they restrict the type of recirculating flow regions that can occur. Their effectiveness, however, can be analysed *a posteriori* when the solution has been computed. Then, for instance, by doubling the length of the diffuser and comparing the solutions, it can be decided how far from the exit the computed results are reliable.

2.3. *Introduction of vorticity and stream function*

The vorticity-stream function formulation of the Navier–Stokes equations has been used. The stream function, Ψ, is introduced satisfying

$$V_r = \frac{1}{rR}\frac{\partial \Psi}{\partial \theta}, \qquad V_\theta = -\frac{1}{R}\frac{\partial \Psi}{\partial r} \tag{2.3}$$

thus ensuring that the continuity equation (2.2) is identically satisfied. The vorticity, ξ, is defined as

$$\xi = (\text{curl } V)\cdot\hat{\phi} \tag{2.4}$$

i.e. the $\hat{\phi}$ component of the vorticity which in the absence of swirl is the only component.

By eliminating pressure in the usual way, the three component equations of (2.1) and equation (2.2) can be re-formulated as three equations in unknowns vorticity, stream function and swirl velocity. The equations may be derived and manipulated into the form

$$\frac{\partial}{\partial r}\left(R^3 r\frac{\partial}{\partial r}\left(\frac{\xi}{R}\right)\right)+\frac{\partial}{\partial\theta}\left(\frac{R^3}{r}\frac{\partial}{\partial\theta}\left(\frac{\xi}{R}\right)\right)-R^2\mathrm{R}\left[\frac{\partial}{\partial r}\left(\frac{\xi}{R}\frac{\partial\Psi}{\partial\theta}\right)-\frac{\partial}{\partial\theta}\left(\frac{\xi}{R}\frac{\partial\Psi}{\partial r}\right)\right]$$
$$= rR\mathrm{R}\left(\frac{\sin\theta}{r}\frac{\partial V_\phi^2}{\partial\theta}-\cos\theta\frac{\partial V_\phi^2}{\partial r}\right) \tag{2.5}$$

$$\frac{\partial}{\partial r}\left(\frac{r}{R}\frac{\partial\Psi}{\partial r}\right)+\frac{\partial}{\partial\theta}\left(\frac{1}{rR}\frac{\partial\Psi}{\partial\theta}\right)=-r\xi \tag{2.6}$$

$$\frac{\partial}{\partial r}\left(R^3 r\frac{\partial}{\partial r}\left(\frac{V_\phi}{R}\right)\right)+\frac{\partial}{\partial\theta}\left(\frac{R^3}{r}\frac{\partial}{\partial\theta}\left(\frac{V_\phi}{R}\right)\right)-\mathrm{R}\left[\frac{\partial}{\partial r}\left(RV_\phi\frac{\partial\Psi}{\partial\theta}\right)-\frac{\partial}{\partial\theta}\left(RV_\phi\frac{\partial\Psi}{\partial r}\right)\right]=0. \tag{2.7}$$

Equations (2.5), (2.6) and (2.7) are referred to as "the vorticity equation", "the stream function equations" and "the swirl velocity equation" respectively.

In the rest of the work, it is convenient to use variables Ω, Ψ and Λ where

$$\Omega=\xi/R\,,\qquad \Lambda=RV_\phi \tag{2.8}$$

and Ψ is as defined earlier. With this choice of variables, all three equations assume the form

$$\frac{\partial}{\partial r}\left(brR\frac{\partial}{\partial r}(c\Phi)\right)+\frac{\partial}{\partial\theta}\left(b\frac{R}{r}\frac{\partial}{\partial\theta}(c\Phi)\right)-a\left[\frac{\partial}{\partial r}\left(\Phi\frac{\partial\Psi}{\partial\theta}\right)-\frac{\partial}{\partial\theta}\left(\Phi\frac{\partial\Psi}{\partial r}\right)\right]=rRd \tag{2.9}$$

where Φ, a, b, c and d are given for the individual equations in table 1.

TABLE 1

Φ	a	b	c	d
Ω	$\mathrm{R}R^2$	R^2	1	$\mathrm{R}R^{-2}\left[\frac{\sin\theta}{r}\frac{\partial\Lambda^2}{\partial\theta}-\cos\theta\frac{\partial\Lambda^2}{\partial r}\right]$
Ψ	0	R^{-2}	1	$-\Omega$
Λ	R	R^2	R^{-2}	0

3. Method of solution

3.1. *The mesh*

A mesh with non-constant spacings has been employed. This allows the use of fine mesh spacings in areas where spatial gradients are large (*e.g.* boundary layers) and relatively coarse mesh spacings where these gradients are small. More effective use of computer time and core-store can then be made than would be possible with a uniform mesh. However, the complexity of the finite difference equations is very much increased and care must be exercised in the construction of the mesh. The ratio of successive mesh spacings should be made as close to unity as possible (especially near walls) and chosen so that the order of magnitude of the truncation error is not impaired [11]. For the mesh systems used by the authors, this ratio varies from 1

at the boundaries to about 1.3 in the middle of the flow passage. The largest mesh spacing is then typically six times as large as the smallest.

3.2. *Finite difference equations*

For the numerical solutions of equations (2.5), (2.6) and (2.7), the method of successive under/over relaxation has been used. No general theory at present exists for satisfactory prediction of the optimum relaxation parameters for non-linear coupled sets of equations. Methods that have proved successful with certain classes of linear equations (*e.g.* [13]) applied to the present equations lead to relaxation parameters that cause divergence. The authors' choice of relaxation parameters ω_1, ω_2 and ω_3 for vorticity, stream function and swirl velocity equations respectively is based on experience and experimental computation. For the majority of calculations, values of ω_1, ω_2 and ω_3 were such that $0.2 \leqq \omega_1 \leqq 0.8$, $0.6 \leqq \omega_2 \leqq 1.5$ and $1.0 \leqq \omega_3 \leqq 1.5$.

The most common way of deriving finite difference equations is by using Taylor Series approximations. Preliminary investigations disclosed that whereas this method is successful for a uniform mesh system, it can lead to severe instabilities with a non-uniform mesh system. It seems likely that the cause of these instabilities could be removed with the use of an appropriate conservative difference scheme. Experimentation with difference equations derived by integration over an elementary area, however, did not reveal any difficulties even with a non-uniform mesh system. An integration method, essentially the same as that used in [12] was therefore adopted. The finite difference representation of (2.9) at point P (see fig. 3) for iteration on k is

$$\Phi_P^{(k+1)} = \Phi_P^{(k)} + \omega[(C_E\Phi_E^{(k)} + C_W\Phi_W^{(k+1)} + C_N\Phi_N^{(k)} + C_S\Phi_S^{(k+1)} - D)/C_P - \Phi_P^{(k)}] \tag{3.1}$$

where

$$\begin{aligned} C_E &= A_E + B_E c_E \\ C_W &= A_W + B_W c_W \\ C_N &= A_N + B_N c_N \\ C_S &= A_S + B_S c_S \\ C_P &= A_E + A_W + A_N + A_S + (B_E + B_W + B_N + B_S)c_P \\ \omega &= \text{relaxation parameter corresponding to } \Phi \end{aligned} \tag{3.2}$$

$$\begin{aligned} A_E &= a_P(\Psi_{SE} + \Psi_S - \Psi_{NE} - \Psi_N + |\Psi_{SE} + \Psi_S - \Psi_{NE} - \Psi_N|)/2 \\ A_W &= a_P(\Psi_{NW} + \Psi_N - \Psi_{SW} - \Psi_S + |\Psi_{NW} + \Psi_N - \Psi_{SW} - \Psi_S|)/2 \\ A_N &= a_P(\Psi_{NE} + \Psi_E - \Psi_{NW} - \Psi_W + |\Psi_{NE} + \Psi_E - \Psi_{NW} - \Psi_N|)/2 \\ A_S &= a_P(\Psi_{SW} + \Psi_W - \Psi_{SE} - \Psi_E + |\Psi_{SW} + \Psi_W - \Psi_{SE} - \Psi_E|)/2 \end{aligned} \tag{3.3}$$

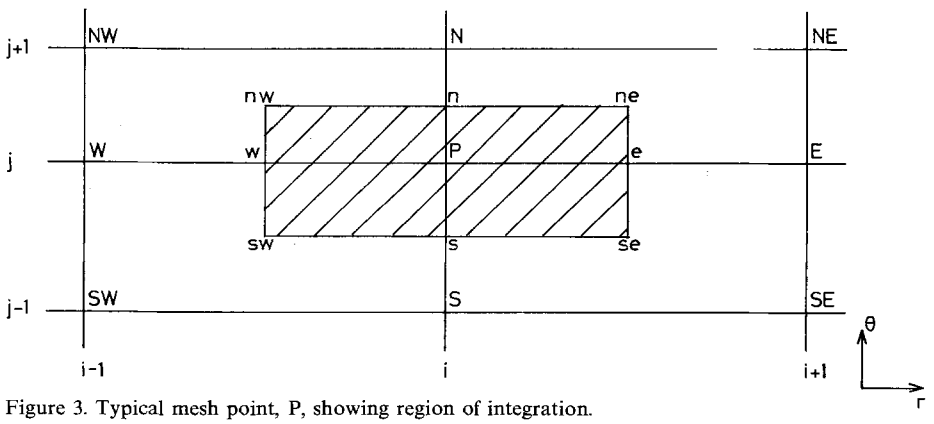

Figure 3. Typical mesh point, P, showing region of integration.

$$
\begin{aligned}
B_E &= (b_E + b_P)(R_E + R_P)(r_E + r_P)(\theta_N - \theta_S)/(16(r_E - r_P)) \\
B_W &= (b_W + b_P)(R_W + R_P)(r_W + r_P)(\theta_N - \theta_S)/(16(r_P - r_W)) \\
B_N &= (b_N + b_P)(r_E - r_W)(R_N + R_P)/(8r_P(\theta_N - \theta_P)) \\
B_S &= (b_S + b_P)(r_E - r_W)(R_S + R_P)/(8r_P(\theta_P - \theta_S)) \\
D &= rRd
\end{aligned}
\tag{3.4}
$$

a, b, c and d are as given in table 1.

One sided difference approximations or "upwind differences" have been used in approximating the convection terms and this results in the convection term coefficients A_E, A_W, A_N and A_S all being positive. Since the B's are also positive, it can be seen that the systems of equations formed for the vorticity and stream function, where the c's are constants, must be diagonally dominant. While it cannot be assured that the system of equations for the swirl is necessarily diagonally dominant, no convergence difficulties have ever been experienced with this system.

Equation (3.1) is applied at each interior point by scanning along lines of constant r systematically in the direction S to N. It is also possible, of course, to scan along lines of constant θ: in fact, all consistent orderings are equivalent [14]. In accordance with the usual S.O.R. theory [15], at this stage $\Phi_P^{(k)}$ is known everywhere and $\Phi^{(k+1)}$ values are used as soon as they are available.

3.3 *Stream function boundary conditions*

Inlet values are calculated from the given inlet radial velocity profile by numerical integration (the Trapezium rule is sufficiently accurate). Since the walls are impermeable, the stream function is a constant on each wall. At the hub boundary the constant is taken to be zero and at the outer wall the value again depends on the inlet flow and gives a measure of the momentum flux. Since the flow is assumed to be radially directed at the exit, the appropriate condition there is

$$
\frac{\partial \Psi}{\partial r} = 0 . \tag{3.5}
$$

3.4. *Swirl velocity boundary conditions*

At the inlet, the swirl velocity profile is assumed to be known. The no-slip condition requires the swirl velocity at the solid walls to be zero unless they are rotating in which case the swirl velocity will be equal to the speed of the wall surface. For swirl induced by rotation of a wall, the appropriate boundary condition is

$$
\frac{\partial V_\phi}{\partial r} = 0 . \tag{3.6}
$$

However, for swirl introduced solely at inlet, equation (3.6) would result in increased angular momentum which is physically impossible. In reality, of course, for this situation the swirl is decaying and the most suitable condition at exit is one that allows the decay rate to be maintained. Such a condition requires

$$
\frac{\partial^2 V_\phi}{\partial r^2} = 0 . \tag{3.7}
$$

3.5. *Vorticity boundary conditions*

The inlet vorticity values are again calculated from the given inlet flow. At the exit the values are determined from the stream function equation simplified by the stream function condition

(3.5). The wall vorticity boundary conditions are the most difficult to deal with. It is believed that the way in which the wall vorticity values are determined is a key factor affecting the accuracy and convergence of the method. Several different formulations have been found for the vorticity on the solid walls of which three have second order truncation errors. Test computer runs with identical data for each of these formulations gave results which were in very close agreement. First order approximations, on the order hand, were found to be hopelessly inadequate. In each case a weighting technique was used to achieve greater stability. The derivation of these various wall vorticity formulae is given in [11]. Here the implementation of one of the second order formulations is illustrated.

$$\Omega_P^{(+1)} = \frac{-2\alpha}{r_P^2 R_P^2} \frac{\theta_2^3(\Psi_{NP}^{(k)} - \Psi_P^{(k)}) - \theta_1^3(\Psi_{NNP}^{(k)} - \Psi_P^{(k)})}{\theta_2^3\theta_1^2 - \theta_1^3\theta_2^2} + (1-\alpha)\Omega_P^{(k)} \tag{3.8}$$

where α is a weighting factor satisfying $0 < \alpha \leqq 1$. Figs. 4a and 4b show the relative positions of points P, NP and NNP for the cases of the hub boundary and wall boundary respectively.

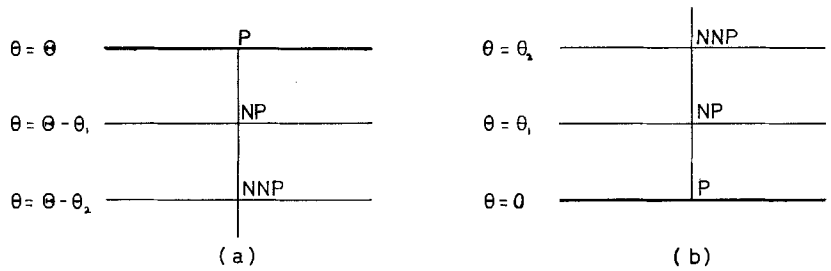

Figure 4. Boundary mesh molecules.

3.6. *Iterative procedure*

Let B denote all boundary mesh nodes and I all interior nodes. The variables to iterate are Ω, Ψ and Λ and after the kth iteration the values obtained are denoted by $\Omega^{(k)}$, $\Psi^{(k)}$ and $\Lambda^{(k)}$. The values at inlet of these main variables are calculated from the given velocity profiles in the straightforward way already indicated. In order to obtain an initial guess, $\Omega^{(0)}$, $\Psi^{(0)}$ and $\Lambda^{(0)}$, the inlet values of these variables are given to all mesh points lying on the same mesh line of constant θ. (Once a solution has been obtained, it can be used as an initial guess for the next case where the Reynolds number is increased.)

The iteration strategy used to find values for $\Omega^{(k+1)}$, $\Psi^{(k+1)}$ and $\Lambda^{(k+1)}$ from the stage where $\Omega^{(k)}$, $\Psi^{(k)}$ and $\Lambda^{(k)}$ are all known, is as follows:

(i) Obtain $\Omega^{(k+1)}$ on I using one S.O.R. cycle and then $\Omega^{(k+1)}$ on B using the appropriate boundary conditions.

(ii) Obtain $\Psi^{(k+1)}$ on I using one S.O.R. cycle. On B, $\Psi^{(k+1)} = \Psi^{(k)}$ except at the exit where new values are found subject to condition (3.5).

(iii) Obtain $\Lambda^{(k+1)}$ on I using one S.O.R. cycle and calculate $\Lambda^{(k+1)}$ at the exit. For the remainder of B, $\Lambda^{(k+1)} = \Lambda^{(k)}$.

(iv) Test to see if

$$\max_{\Phi=\xi,\Psi,\Lambda} \left[\max_{\substack{B+I \\ |\Phi^{(k)}|>10^{-3}}} \left| \frac{\Phi^{(k)} - \Phi^{(k+1)}}{\Phi^{(k)}} \right| \right] < \varepsilon .$$

(v) If the convergence criterion (iv) is satisfied the values of $\Omega^{(k+1)}$, $\Psi^{(k+1)}$ and $\Lambda^{(k+1)}$ are taken as the solution, otherwise the iteration process continues.

It is possible to devise any number of iterative strategies but what the optimum strategy is seems to be an open question. After a limited amount of experimentation, the method outlined above was adopted where only one iteration of each variable is performed before progressing to the next.

4. Diffuser performance calculations

The usual parameter for rating diffusers is the pressure recovery coefficient, defined as the static pressure rise through the diffuser normalised on the inlet dynamic head. The pressure distribution in the diffuser must therefore be found. Equations for the pressure derivatives $\partial P/\partial r$ and $\partial P/\partial\theta$ can be found in terms of the calculated flow variables from the $\hat{r}$ and $\hat{\theta}$-component equations of (2.1) respectively. For the present co-ordinate system these equations are rather involved but consideration of the total head, $H=P+\frac{1}{2}V^2$ leads to a formulation that can be handled more conveniently

$$\begin{aligned}\frac{\partial H}{\partial r} &= -\frac{\partial \Psi}{\partial r}\Omega + \frac{1}{2R^2}\frac{\partial \Lambda^2}{\partial r} - \frac{1}{rR\mathrm{R}}\frac{\partial}{\partial\theta}(R^2\Omega)\\ \frac{\partial H}{\partial\theta} &= -\frac{\partial \Psi}{\partial\theta}\Omega + \frac{1}{2R^2}\frac{\partial \Lambda^2}{\partial\theta} + \frac{r}{R\mathrm{R}}\frac{\partial}{\partial r}(R^2\Omega)\end{aligned} \tag{4.1}$$

where

$$\Lambda = RV_\phi \text{ and } \Omega = \xi/R\,.$$

Since the distributions for Ω, Ψ and Λ are known, (4.1) are sufficient to calculate pressure differences uniqely.

It was found that in order to attain second order accuracy for the pressure distribution, an iterative method of solution was necessary. Furthermore, difficulties arise as a result of having used upwind differences in the solution for the main variables. However, consistency in the sense that pressure integrals round closed contours should be zero, could be attained by using upwind differences for the pressure calculation. Details of the calculation method are given in [11]. The convergence criterion for the pressure iteration was chosen so that further reduction of the residuals would not affect the efficiency of the diffuser. It should be noted that the efficiency is a very sensitive parameter.

The *pressure recovery coefficient*, C_{P}, is obtained by comparing the actual static pressure rise through the diffuser in question with the static pressure rise theoretically obtainable for complete diffusion and ideal flow, (i.e. the static pressure rise normalised on the inlet kinetic energy).

The *ideal pressure recovery coefficient*, $C_{\mathrm{P_i}}$, is the C_{P} value that would result were the flow ideal.

The *diffuser efficiency*, E, compares the static pressure rise obtained with the theoretical static pressure rise for the given diffuser were the flow ideal.

In calculating diffuser performance parameters for non-swirling flows it is often assumed that the static pressure and velocity are constant across inlet and exit. For boundary layer methods the pressure rise is then determined by applying Bernoulli's equation to the potential core together with a conservation of mass equation (*e.g.* [7] and [16]). However, substantial non-uniformities are produced when separation occurs or for swirling flows where there is a pressure gradient normal to the main flow direction. The difficulty now arises of what averaging procedure to use in order to calculate performance parameters. Two methods that have been used (usually in experimental work) are:

(i) mass flow averaging with corresponding parameter C_{PM} *e.g.* [5] and [17],

(ii) area averaging giving rise to parameter C_{PA} *e.g.* [2], [4] and [18].

In non-dimensional terms for the present situation

$$C_{PM} = \left(\int_{A_2} P_2 V_{r_2} dA_2 - \int_{A_1} P_1 V_{r_1} dA_1\right) \Big/ \int_{A_1} \tfrac{1}{2}V_1^2 V_{r_2} dA_1 \tag{4.2}$$

and

$$C_{PA} = \left(\frac{A_1}{A_2}\int_{A_2} P_2 dA_2 - \int_{A_1} P_1 dA_1\right) \Big/ \int_{A_1} \tfrac{1}{2}V_1^2 dA_1 \tag{4.3}$$

where A_1 and A_2 are respectively the areas of inlet and exit annular surfaces and the suffix 1 refers to inlet values while suffix 2 indicates exit values. The surfaces A_1 and A_2 are surfaces of constant r. (For small θ these surfaces do not deviate much from the corresponding plane surfaces normal to the axis of symmetry.) It is felt that when pressures and velocities are significantly non-uniform across inlet and exit, the mass flow averaging formula (4.2) based on the concept of flow energy is the most appropriate.

For ideal flow with no "total pressure" losses

$$\int_{A_1} P_1 \tilde{V}_{r_1} dA_1 + \int_{A_1} \tfrac{1}{2}\tilde{V}^2 \tilde{V}_{r_1} dA_1 = \int_{A_2} P_2 \tilde{V}_{r_2} dA_2 + \int_{A_2} \tfrac{1}{2}\tilde{V}^2 \tilde{V}_{r_2} dA_2 \tag{4.4}$$

where $\tilde{V}$, $\tilde{V}_1$, $\tilde{V}_2$ *etc.* indicate velocities for ideal flow. Using (4.4) to eliminate P_2 in (4.2) leads to an expression for the ideal pressure recovery C_{PM_i}

$$C_{PM_i} = 1 - \left\{ \int_{A_2} \tfrac{1}{2}\tilde{V}_2^2 \tilde{V}_{r_2} dA_2 \Big/ \int_{A_1} \tfrac{1}{2}\tilde{V}_1^2 \tilde{V}_{r_1} dA_1 \right\}. \tag{4.5}$$

Correspondingly, for area averaged ideal flow

$$\int_{A_1} P_1 dA_1 + \int_{A_1} \tfrac{1}{2}\tilde{V}_1^2 dA_1 = \frac{A_1}{A_2} \int_{A_2} P_2 dA_2 + \frac{A_1}{A_2} \int_{A_2} \tfrac{1}{2}\tilde{V}_2^2 dA_2 \tag{4.6}$$

which in conjunction with (4.3) gives

$$C_{PA_i} = 1 - \left(\frac{A_1}{A_2} \int_{A_2} \tfrac{1}{2}\tilde{V}_2^2 dA_2 \right) \Big/ \left(\int_{A_1} \tfrac{1}{2}\tilde{V}_1^2 dA_1 \right). \tag{4.7}$$

Taking $\tilde{V} = (\tilde{V}_r, 0, 0)$ and replacing $\tilde{V}_r$ by its average over the relevant surface, both C_{PM_i} and C_{PA_i} reduce to the usual ideal pressure recovery formula [16], [19]

$$C_{P_i} = 1 - (AR)^{-2} \tag{4.8}$$

where AR = area ratio $= A_2/A_1$. Equation (4.8) takes no account of nonuniformities in the velocity profiles and the corresponding additional energy. It is possible in certain circumstances for its use to result in theoretical efficiencies in excess of 100% (*e.g.* a highly non-uniform inlet flow under favourable circumstances resulting in uniform exit flow).

As mentioned earlier, A_1 and A_2 are taken as annular surfaces of constant r. It is convenient to denote by Θ and θ_h (usually zero) the θ-values of the outer casing and hub respectively so that

$$\begin{aligned} A_1 &= \int_{A_1} dA_1 = \int_{\theta_h}^{\Theta} 2\pi R_1 r_1 d\theta \\ A_2 &= \int_{A_2} dA_2 = \int_{\theta_h}^{\Theta} 2\pi R_2 r_2 d\theta \end{aligned} \tag{4.9}$$

where

$$R_i = a + r_i \sin\theta \qquad (i = 1, 2).$$

Equation (4.2) can then be re-written as

$$C_{PM} = \frac{\displaystyle\int_{\theta_h}^{\Theta} P_2 V_{r_2} R_2 r_2 d\theta - \int_{\theta_h}^{\Theta} P_1 V_{r_1} R_1 r_1 d\theta}{\displaystyle\int_{\theta_h}^{\Theta} \tfrac{1}{2} V_1^2 V_{r_1} R_1 r_1 d\theta}. \tag{4.10}$$

Similarly, C_{PA}, C_{PM} and C_{PA}, can be formulated in terms of integrals involving the θ co-ordinates.

The parameters C_{PM} and C_{PA} are expressed in terms of integrals of quantities that are known

at all mesh points. The mesh is sufficiently refined for the integrations to be carried out accurately using the trapezium rule.

The diffuser efficiencies E_M and E_A are calculated from

$$E_M = C_{PM}/C_{PM_i}, \quad E_A = C_{PA}/C_{PA_i}. \tag{4.11}$$

It remains now to find suitable expressions for V_2 in (4.5) and (4.6) so that the ideal pressure recoveries can be calculated. These ideal pressure recovery coefficients should represent a valid upper limit on the actual pressure recovery coefficient. The velocity at inlet $\tilde{V}_1 = (\tilde{V}_{r_1}, 0, \tilde{V}_{\phi_1})$ is known. For radially directed axially symmetric flow, the continuity equation (2.2) gives

$$\begin{aligned} &rRV_r = \text{const.} \qquad \theta_h \leqq \theta \leqq \Theta \\ &r_1(a+r_1 \sin\theta)V_{r_1} = r_2(a+r_2 \sin\theta)V_{r_2} \qquad \theta_h \leqq \theta \leqq \Theta. \end{aligned} \tag{4.12}$$

This enables an exit radial velocity profile to be found that satisfies mass conservation. In order to find the swirl distribution at exit, use is made of Kelvin's circulation theorem; *viz.* 'for ideal flow the circulation round any closed curve C moving with the fluid is a constant'. *i.e.*

$$\text{Circulation} = \int_{\text{circuit at inlet}} V_1 \cdot ds_1 = \int_{\text{corresponding circuit at exit}} V_2 \cdot ds_2$$

Taking in each case the circuit for a constant θ-value gives

$$\int_0^{2\pi} V_{\phi_1} R_1 \, d\phi = \int_0^{2\pi} V_{\phi_2} R_2 \, d\phi$$

whence from axial symmetry

$$V_{\phi_2} = \frac{R_1}{R_2} V_{\phi_1}. \tag{4.13}$$

Once the exit distribution of swirl and radial velocity has been found C_{PM_i} and C_{PA_i} are calculated by numerical integration.

5. Summary and comments

The great advantage of the co-ordinate system used is that physical boundaries correspond to surfaces of constant θ or constant r, thus simplifying the numerical analysis. However, for a realistic number of mesh points, core store problems arise. The diffusion coefficients (equation 3.4) are constant throughout the iteration procedure and should therefore be calculated and stored. Thus for each variable at each interior mesh point it is necessary to store B_N, B_S, B_E and B_W. For a grid system of 1,000 mesh points, for example, 24k words of core store would be required for these coefficients alone. In spherical polar co-ordinates the problem can be overcome at the expense of a single multiplication each time a coefficient is used since

$$B_x(\theta, r) = f_x(r) g_x(\theta), \qquad (x = \text{N, S, E, or W}) \tag{5.1}$$

and so, for example

$$B_E[i, j] = f_E[i] \, g_E[j], \qquad (1 \leqq i \leqq \text{N1}, 1 \leqq \text{N2}).$$

Each coefficient then requires only N1 + N2 numbers to be stored rather than N1 × N2. For the co-ordinate system used here, a decomposition of the form (5.1) is not possible because of the presence of the a in $R = a + r \sin\theta$. Three alternatives for the coefficients B are possible:

(i) Store all the coefficients at each mesh point.

(ii) Work out the coefficients afresh each time they are needed.

(iii) Store the coefficients on disc and bring them into the fast access core only when needed.

Alternative (i) leads to a larger core-store requirement than was available while (ii) is time consuming and inefficient and so alternative (iii) was adopted even though it calls for disc transfers at each iteration of each variable.

Difficulties in obtaining convergence for this type of problem for moderate and high Reynolds number, have led to the widespread use of the one sided difference approximations for convective terms known appropriately as "Upwind Differences". This type of approximation ensures a diagonally dominant iteration matrix and hence better convergence characteristics. Even so, under-relaxation, as used in [20] in the absence of "Upwind Differences", is still necessary for convergence in most cases. The theory of second order linear partial differential equations, which has reached a high stage of sophistication regarding prediction of optimum overrelaxation parameters, is virtually useless here and in general, experience is the only guide. The equation that presents most difficulty is the vorticity equation for which the relaxation parameter was sometimes reduced to 0.2. The stream function equation is also under-relaxed in many cases, but the swirl velocity equation presents few problems and could always be over-relaxed. There appears to be a coupling effect between the relaxation parameter for the vorticity and the stream function. It was found that increasing the stream function relaxation parameter requires the vorticity relaxation parameter to be decreased if convergence is to be achieved.

Solutions for low Reynolds number cases are not usually difficult to obtain. However, unless the initial guess for high Reynolds number cases is sufficiently close to the true solution, obtaining convergence can be most difficult. For this reason, once a solution has been obtained, it is used as the initial guess for the next higher Reynolds number case. As will be mentioned in Part II, there is sometimes a critical combination of swirl and Reynolds number where the flow regime changes. For cases close to this situation, convergence can be very slow indeed.

The computer program is sufficiently versatile (subject to convergence considerations) to deal with arbitrary inlet radial velocity profile and any combination of inlet swirl, hub swirl and outer wall swirl. Any straight walled axially symmetric annular geometry where the hub wall and outer wall would intersect if produced backwards can be considered. Also within the scope of the program is the special case where the hub shrinks to zero leaving a conical diffuser.

The method that has been discussed is capable of predicting laminar flow through straight-walled annular diffusers. Extensions of this work must incorporate a suitable turbulence model. In this connection the work on turbulence of Spalding *et al.* at Imperial College and Harlow *et al.* at Los Alamos looks most encouraging.

REFERENCES

[1] G. Sovran and E. Klomp, Experimentally determined optimum geometries for rectilinear diffusers with rectangular, conical or annular cross-section, *Fluid Mechanics of Internal Flow*, Elsevier (1969) 270–319.

[2] S. J. Kline, D. E. Abbott and R. W. Fox, Optimum design of straight walled diffusers, *J. Basic Eng.*, 81 (1959) 321–329

[3] F. A. L. Winternitz and W. J. Ramsay, Effects of inlet boundary layer on pressure recovery, energy conversion and losses in conical diffusers, *J' Roy. Aero. Soc.*, 61 (1957) 116–124.

[4] A. T. McDonald, R. W. Fox and R. V. Van Dewoestine, *Effects of swirling inlet flow on pressure recovery in conical diffusers*, AIAA paper no. 71–84 (1971) 1–9.

[5] D. Hoadley, *Some measurements of swirling flow in an annular diffuser*, Report W/M(3E) p. 1621. M. E. L. Whetstone. English Electric Co., Ltd. (1970).

[6] H. Schlichting and K. Gerstan, Calculation of the flow in rotationally symmetric diffusers with the aid of boundary layer theory, *Z. Flugwiss* 9 (1961) 135–140.

[7] H. E. Imbach, Calculation of rotationally symmetrical turbulent flow through diffusers, *The Brown Boveri Review*, 51 (1964) 789–801.

[8] A. D. Carmichael and G. N. Pustintsev, Prediction of turbulent boundary layer development in conical diffusers, *J. Mech. Eng. Sci.*, 8 (1966) 426–436.

[9] J. H. Horlock and R. I. Lewis, Shear flows in straight-sided nozzles and diffusers, *Int. J. Mech. Sci.*, 2 (1961) 251–266.

[10] Y. Furuya, Experiments and theory on flow in a diffuser, *Mem. Fac. Eng. Nayoya Univ.*, 10 (1958) 1–41.

[11] C. M. Crane, *Numerical solution of the Navier–Stokes equations with particular reference to the effects of swirl*, Ph.D. thesis, the University of Sheffield (1972).

[12] A. D. Gosman, W. M. Pun, A. K. Runchal, D. B. Spalding and M. W. Wolfstein, *Heat and mass transfer in recirculating flows*, Academic Press (1969).

[13] B. A. Carré, The determination of the optimum accelerating factor for successive over-relaxation, *The Computer Journal* 4 (1961) 73–78.

[14] R. S. Varga, Orderings of the successive overrelaxation scheme, *Pacific Journal of Mathematics*, 9 (1959) 925–939.
[15] R. S. Varga, *Matrix iterative analysis*, Prentice-Hall Inc. (1962).
[16] L. R. Reneau and J. P. Johnston, A performance prediction method for unstalled, two-dimensional diffusers, *J. Basic Eng.*, 89 (1967) 643–654.
[17] H. Peters, Conversion of energy in cross-section divergencies under different conditions of inflow, *Ing. Archiv*, 2 (1931) 92–107, Translation N.A.C.A. T.M. 737 (1934).
[18] B. A. Waitman, L. R. Reneau and S. J. Kline, Effects of inlet conditions on performance of two-dimensional subsonic diffusers, *J. Basic Eng.*, 83 (1961) 349–360.
[19] D. J. Cockrell and E. Markland. A review of incompressible diffuser flow, *Aircraft Engineering*, 35 (1963) 286–292.
[20] O. R. Burggraf, Analytical and numerical studies of the structure of steady separated flows, *J. Fluid Mech.*, 24 (1966) 113–151.